Article

Current Biology

Hormonal coordination of motor output and internal prediction of sensory consequences in an electric fish

Graphical abstract

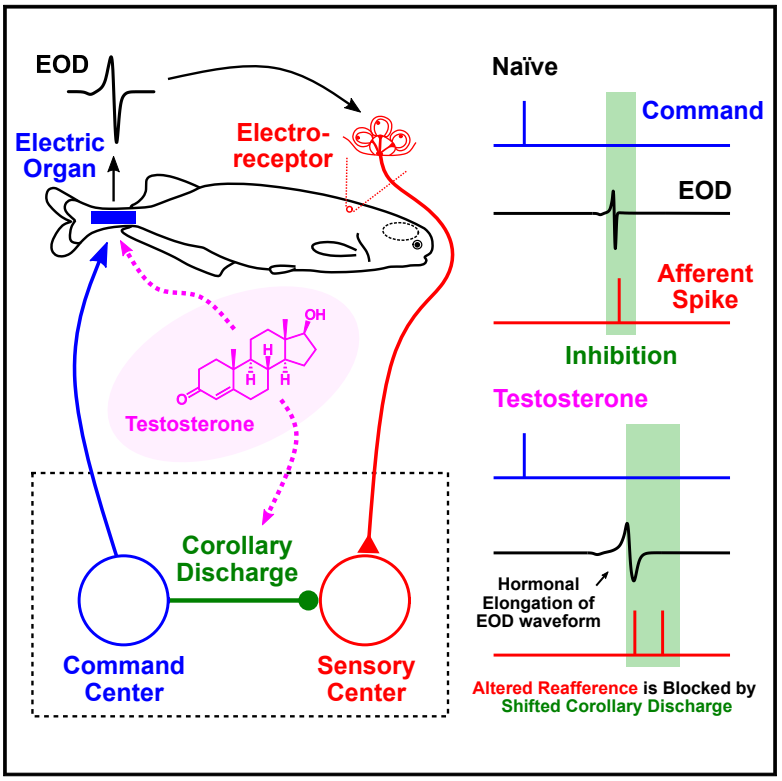

Authors

Matasaburo Fukutomi, Bruce A. Carlson

Correspondence

carlson.bruce@wustl.edu

In brief

Steroid hormones alter behavior, but animals still need to distinguish between self- and other-generated stimuli. Using electric fish, Fukutomi and Carlson show that testosterone independently regulates electric signals and corollary discharge timing, maintaining a match between the sensory consequences of behavior and their central cancelation.

Highlights

- Testosterone elongates electric pulses, altering the resulting sensory feedback
- Testosterone delays and elongates the time window of corollary discharge inhibition
- Hormonally shifted corollary discharge timing matches the shifted reafferent input
- Sensory feedback is not necessary to induce hormonal shift of corollary discharge

Fukutomi & Carlson, 2023, Current Biology *33*, 3350–3359
August 21, 2023
https://doi.org/10.1016/j.cub.2023.06.069

CellPress

CellPress

Current Biology

Article

Hormonal coordination of motor output and internal prediction of sensory consequences in an electric fish

Matasaburo Fukutomi[1,2] and Bruce A. Carlson[1,3,4,*]
[1]Department of Biology, Washington University in St. Louis, St. Louis, MO 63130, USA
[2]Twitter: @mata_fukutomi
[3]Twitter: @BruceCarlson75
[4]Lead contact
*Correspondence: carlson.bruce@wustl.edu
https://doi.org/10.1016/j.cub.2023.06.069

SUMMARY

Steroid hormones remodel neural networks to induce seasonal or developmental changes in behavior. Hormonal changes in behavior likely require coordinated changes in sensorimotor integration. Here, we investigate hormonal effects on a predictive motor signal, termed corollary discharge, that modulates sensory processing in weakly electric mormyrid fish. In the electrosensory pathway mediating communication behavior, inhibition activated by a corollary discharge blocks sensory responses to self-generated electric pulses, allowing the downstream circuit to selectively analyze communication signals from nearby fish. These pulses are elongated by increasing testosterone levels in males during the breeding season. We induced electric-pulse elongation using testosterone treatment and found that the timing of electroreceptor responses to self-generated pulses was delayed as electric-pulse duration increased. Simultaneous recordings from an electrosensory nucleus and electromotor neurons revealed that the timing of corollary discharge inhibition was delayed and elongated by testosterone. Furthermore, this shift in the timing of corollary discharge inhibition was precisely matched to the shift in timing of receptor responses to self-generated pulses. We then asked whether the shift in inhibition timing was caused by direct action of testosterone on the corollary discharge circuit or by plasticity acting on the circuit in response to altered sensory feedback. We surgically silenced the electric organ of fish and found similar hormonal modulation of corollary discharge timing between intact and silent fish, suggesting that sensory feedback was not required for this shift. Our findings demonstrate that testosterone directly regulates motor output and internal prediction of the resulting sensory consequences in a coordinated manner.

INTRODUCTION

Steroid hormones underlie seasonal or developmental changes in animal behavior, such as the seasonal songs of birds and the lowering of the voice in humans through secondary sexual characteristics. Such behavioral shifts are based on direct effects of hormones at multiple sites, including peripheral effectors,[1–4] central motor circuits,[5–7] and sensory systems.[8–10] Because these elements are closely interrelated, hormonal changes in behavior likely require coordinated changes in sensorimotor integration. However, little is known about the hormonal control of sensorimotor integration. Here, we investigate hormonal effects on a corollary discharge that provides motor information to modulate central sensory processing in weakly electric mormyrid fish. In this system, mechanisms of corollary discharge and hormonal effects on motor output are well understood.

Mormyrid fish generate electric pulses by discharging an electric organ in their tail[11] (Figure 1A). These pulses are used for active electrolocation[12] and communication.[13] The waveform of the electric organ discharge (EOD) is stereotyped to represent the sender's identity, such as species, sex, and social status,[1,14–16] while the interval between EODs can be flexibly varied to communicate behavioral states in the moment.[17–19] Mormyrids have a dedicated sensory pathway for processing electric communication signals[20–22] in which a corollary discharge plays an essential role.[23,24] In this pathway, the primary sensory center (the nucleus of the electrosensory lateral line lobe [nELL]) receives two types of inputs: excitation from sensory afferents of electroreceptors (knollenorgan [KO]) distributed throughout the surface of the skin, and inhibition originating from the EOD command nucleus (CN) in the medulla through a corollary discharge pathway[21,23–26] (Figure 1B). Both self- and other-generated EODs stimulate KOs, but this internal inhibitory signal precisely blocks sensory responses to self-generated EODs, allowing the downstream pathway to selectively process sensory information from the EODs emitted by nearby fish (Figure 1B).

This communication system is sensitive to the steroid hormone testosterone.[27] Exogenous administration of testosterone increases EOD duration in juveniles, females, and non-reproductive

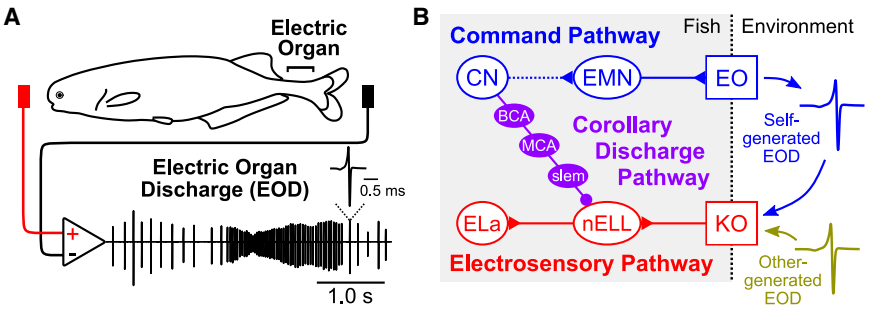

Figure 1. Electric signaling behavior and the sensorimotor circuit of mormyrid fish

(A) Electrical recording from a freely swimming mormyrid, *Brienomyrus brachyistius*. Electric signaling consists of a fixed waveform and variable inter-pulse intervals of electric organ discharge (EOD). The changes in EOD amplitude are due to movement of the fish relative to the recording electrode, not to changes in EOD amplitude emitted by the fish. If the recording electrode (red) is placed on the head side and the reference electrode (black) on the tail side, then a head-positive waveform will be recorded.

(B) Circuit diagram showing electromotor command (blue), knollenorgan (KO) electrosensory (red), and corollary discharge (purple) pathways. The command nucleus (CN) drives the electric organ (EO) to generate each EOD via the medullary relay nucleus (MRN, not shown) and spinal electromotor neurons (EMNs). KO electroreceptors respond to both self- and other-generated EODs and send time-locked spikes to the first center (the nucleus of the electrosensory lateral line lobe [nELL]) via primary afferents. The CN sends corollary discharge inhibition to the nELL via the bulbar command-associated nucleus (BCA), the mesencephalic command-associated nucleus (MCA), and the sublemniscal nucleus (slem), which blocks sensory responses to self-generated EODs. This circuit allows the nELL neurons to send filtered sensory information about EODs generated by other fish to the anterior exterolateral nucleus (ELa).

males, mimicking the sexual differentiation of mature males that occurs during the breeding season.[1] In this case, testosterone directly affects the biophysical properties of the electrocytes in the electric organ that determine the EOD waveform.[11,28–30] Testosterone also induces a downward shift in the sensory tuning of the KOs to match the spectral content of the altered EOD, but this hormonal effect is indirect and depends on sensory feedback.[31] If the sensory feedback (or reafferent input) changes, then the timing of corollary discharge inhibition would also need to change in concert to continue filtering out responses to self-generated EODs. Indeed, a previous study comparing different species of mormyrids showed that fishes with long EODs have delayed corollary discharge inhibition compared with those with short EODs.[32] This difference in the timing of inhibition optimally matches the timing of reafferent input from KOs, which differs between species.[32] Furthermore, this trend was observed for individual differences in EOD duration within one species.[32]

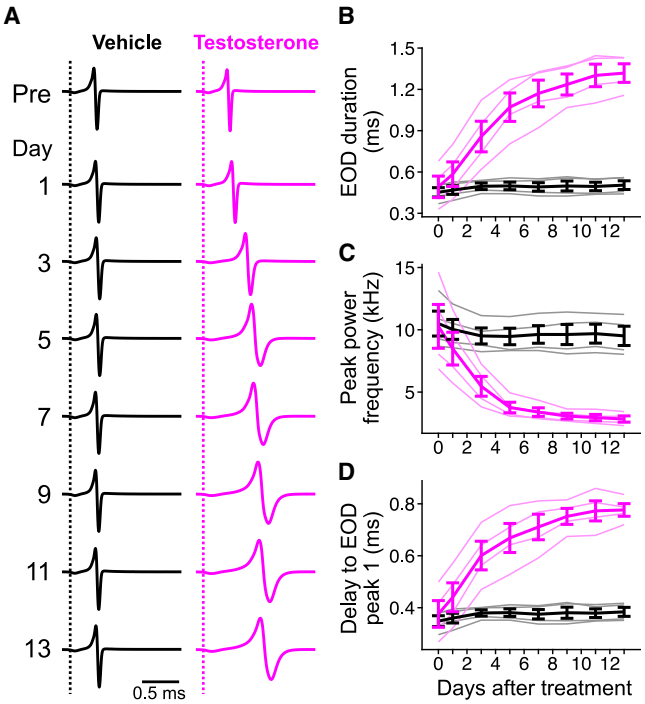

Figure 2. EOD duration is elongated by testosterone treatment

(A) Daily changes in EOD waveform in response to vehicle (black) and testosterone (magenta) treatment. Dotted line indicates EOD onset, determined as the point crossing 20% of peak-0 amplitude (see STAR Methods).

(B–D) Daily changes in EOD duration (B), peak power frequency (C), and delay to EOD peak 1 (D). Each light-color line indicates individual fish (n = 4 fish for each treatment) and dark-color line indicates the average. Error bars indicate SEM.

In the present study, using testosterone treatment, we first quantify a hormonally induced shift in reafferent input by recording individual EOD waveforms and KO spiking responses to a mimic of the fish's own EOD. Then, we show that the timing of corollary discharge inhibition is also altered by testosterone to match the shifted reafferent input. Lastly, we ask how this matching is accomplished. We surgically silenced fish to remove the effect of sensory feedback during hormone treatment and show that the hormonal shift in corollary discharge occurs similarly in both silent and intact fish. Our results demonstrate that testosterone directly regulates electromotor output and corollary discharge in a coordinated manner.

RESULTS

Testosterone elongates EOD duration

We recorded individual EODs of freely swimming fish from the start of treatment to 13 days after treatment (Figure 2A). Testosterone treatment increased EOD duration, while the vehicle treatment had no effect (Figure 2B; $p = 0.0008$ for treatment, $p < 0.0001$ for days after treatment, $p < 0.0001$ for the interaction, linear mixed model [LMM]). Accordingly, peak power frequencies of the EODs were lowered by the testosterone treatment (Figure 2C; $p = 0.0020$ for treatment, $p < 0.0001$ for days after treatment, $p < 0.0001$ for the interaction, LMM). These results were consistent with previous studies.[1,29,30] The EOD waveform of *Brienomyrus brachyistius* is triphasic: the first small head-negative peak, the second large head-positive peak, and the third large head-negative peak are referred to as peak 0,

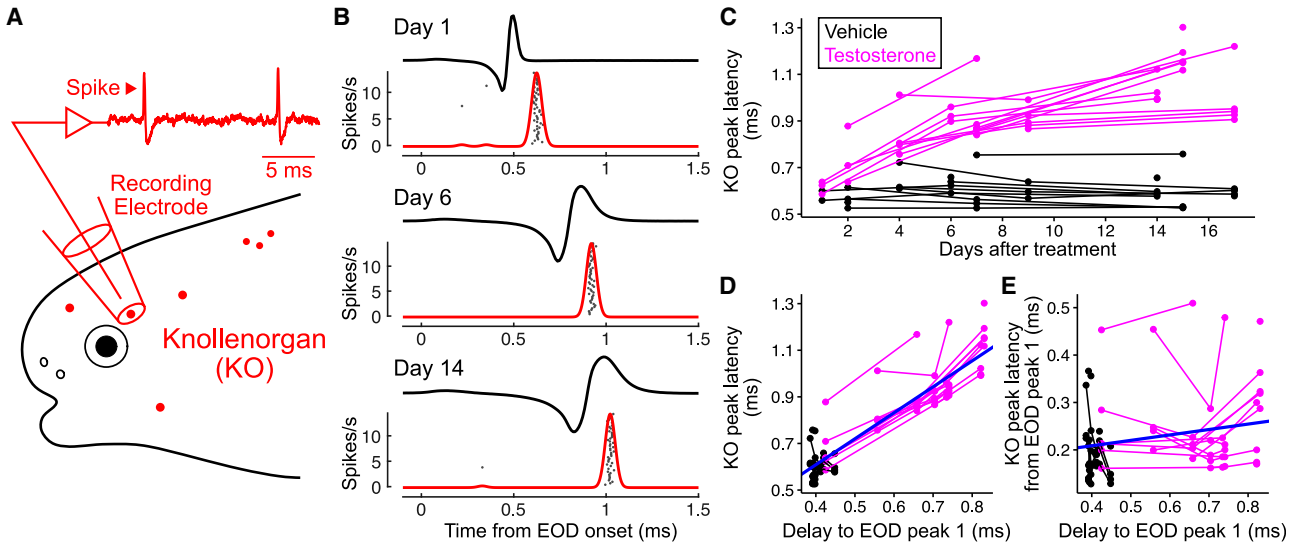

Figure 3. The timing of reafferent spikes from KO electroreceptors is shifted by EOD elongation through testosterone treatment

(A) Schematic representation of electrophysiological recording from KOs. Recording electrode is positioned over an individual KO without touching it.

(B) Example traces in response to self-generated EODs recorded from an identical KO of a testosterone-treated fish at 1, 6, and 14 days after treatment. Inverted EOD waveform recorded from the same fish on the same day was used for sensory stimulation. Spike rate was calculated using a spike density function (see STAR Methods). Raster plots show spike timing over 50 repetitions.

(C) Daily changes in KO peak latency by vehicle (black) and testosterone (magenta) treatment. Each line connects points that correspond to the same KO recorded across multiple days (34 recordings from 16 KOs for vehicle treatment and 38 recordings from 16 KOs for testosterone treatment).

(D) Relationship between delay to EOD peak 1 and KO peak latency. Regression line (blue) was determined using a linear mixed-effect model. The slope is 1.11, and the intercept is 0.16.

(E) Relationship between delay to EOD peak 1 and KO peak latency to EOD peak 1. The slope is 0.11, and the intercept is 0.16.

See also Figure S1.

peak 1, and peak 2, respectively. Delay to peak 1 of the self-generated EOD is strongly correlated with KO receptor spike timing.[32] We confirmed that testosterone treatment also increased the delay to EOD peak 1 (Figure 2D; $p = 0.0009$ for treatment, $p < 0.0001$ for days after treatment, $p < 0.0001$ for the interaction, LMM).

EOD elongation shifts KO spike timing

We recorded spiking activity from KOs of treated fish in response to electrosensory stimulation that mimics a self-generated EOD (Figure 3A; see STAR Methods). A representative KO produced a single spike with short delay following peak 1 of the EOD and was found to shift its spike timing along with testosterone-induced EOD elongation (Figure 3B). Across KOs, we found that testosterone shifted the peak response latency (Figure 3C; $p < 0.0001$ for treatment, $p < 0.0001$ for days after treatment, $p < 0.0001$ for the interaction, LMM). A linear regression comparing KO response latency with the delay to EOD peak 1 revealed a strong correlation, with a slope of 1.11 and intercept of 0.16 (Figure 3D; $p < 0.0001$ for slope, $p < 0.0001$ for intercept, LMM). We also measured the correlation between KO peak latency and delay to EOD peak 1 and found a slope of 0.11, which was significantly larger than 0 (Figure 3E; $p = 0.033$ for slope, LMM), indicating that KO spike latency relative to EOD peak 1 also slightly increased as the EOD elongated.

KOs typically emit a single spike with a fixed delay relative to EOD peak 1,[32,33] but our recordings included several KOs that had a relatively strong second peak in their average firing rate (or spike density function; see STAR Methods) (Figure S1A). We counted KOs with a second peak whose Z score was greater than 3 and whose timing was within 5 ms of EOD onset and found more testosterone-treated KOs (Figure S1B, 5/16 total KOs, 9/38 total responses over multiple days) in this range than vehicle-treated KOs (Figure S1B, 1/16 total KOs, 1/34 total responses). These second peaks resulted from either (1) multiple spikes to a single EOD stimulus or (2) a single spike with variable timing across trials.

Overall, these results suggest that reafferent input to the KO sensory pathway can be altered by testosterone treatment, which may require coordinated changes to corollary discharge timing to inhibit it effectively.

Testosterone shifts corollary discharge timing

To measure the inhibitory effect of corollary discharge in the KO pathway, we recorded evoked potentials from the anterior exterolateral nucleus (ELa) in the midbrain, which is the main target of nELL projection axons (Figure 1B). In this preparation, neuromuscular paralysis blocks EOD production while spontaneous EOD commands (EODCs) remain, leaving the corollary discharge effects on sensory processing intact.[24] We stimulated with 0.2-ms bipolar square electric pulses delivered with a specific delay, typically between 0.2 and 10.2 ms after the EODC, recorded from spinal electromotor neurons (EMNs) (Figure 4A). Electrosensory responses of a vehicle-treated fish were blocked for a narrow range of stimulus delays (~3–4 ms) following the EODC due to the corollary discharge inhibition in nELL

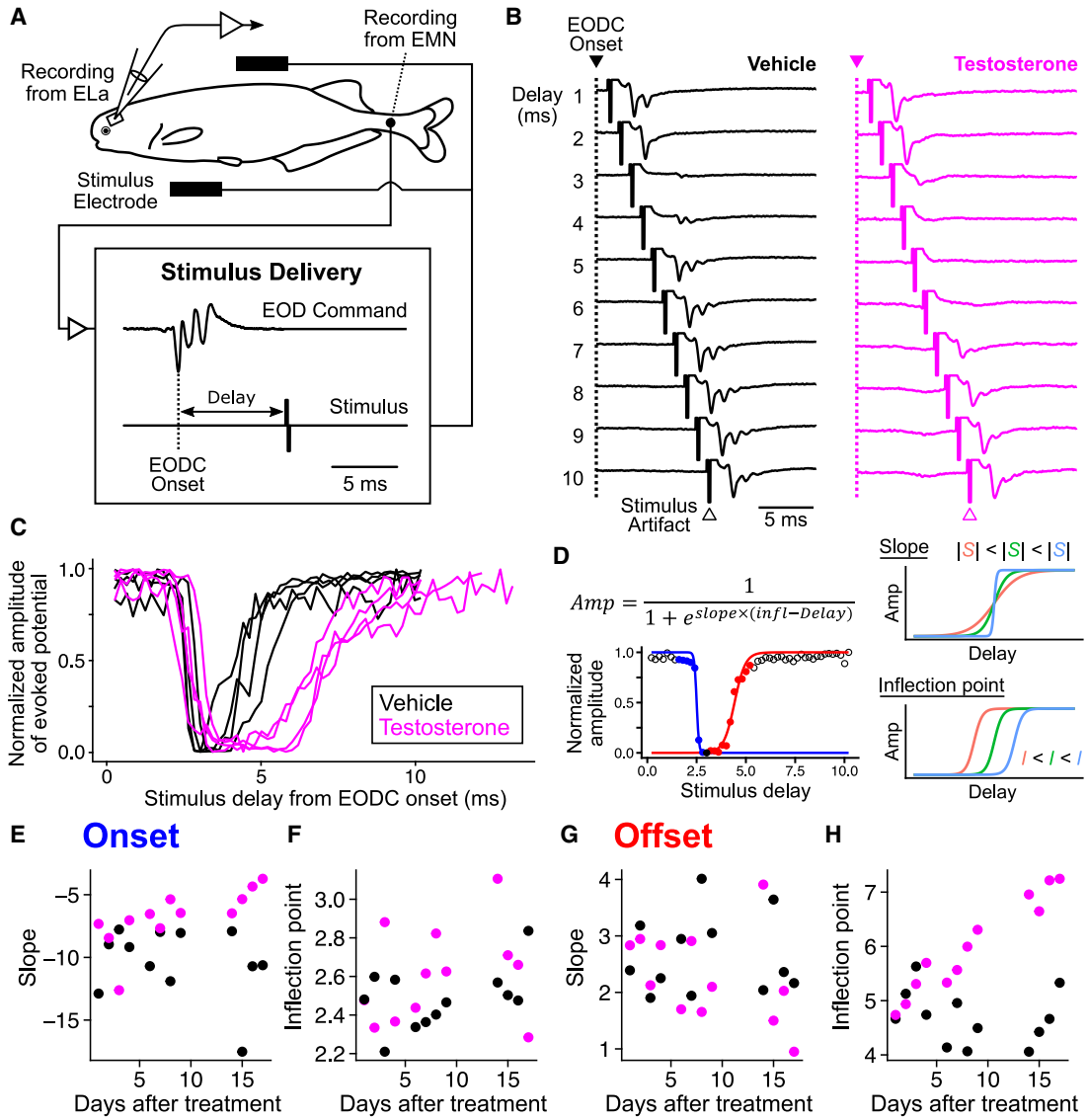

Figure 4. Corollary discharge timing is altered by testosterone treatment

(A) Measurement of corollary discharge timing. Although the fish is curarized to eliminate movement and silence EOD production, EOD commands (EODCs) from spinal electromotor neurons (EMNs) can be recorded as fictive EODs. Electrosensory stimuli can be delivered at fixed delays relative to the EODC onset, which is determined as the first negative peak, while recording evoked potentials in ELa.

(B) Representative mean evoked potentials in response to stimuli at varying delays following the EOD command (1–10 ms) in vehicle- and testosterone-treated fish recorded 16 days after treatment.

(C) Corollary discharge inhibition curves in vehicle- and testosterone-treated fish recorded 14–17 days after treatment. Normalized amplitudes were calculated using the maximum and minimum peak-to-peak amplitude across all stimulus delays.

(D) Sigmoid curve fitting. On the left is the expression used and an example of an inhibition tuning curve fitted to separate onset and offset sigmoid curves. The filled black circle is the minimum point, with the left side defined as the onset direction and the right side as the offset direction. Filled colored circles are data points used for each sigmoid fit (blue, onset; red, offset). On the right is a description of how the coefficients, slope, and inflection point are related to the shapes of the curves.

(E–H) Changes in onset slope (E), inflection point of the onset (F), offset slope (G), and inflection point of the offset (H). Each circle indicates individual fish (n = 12 for each treatment).

(Figure 4B, left), as shown previously.[32] Strikingly, the window over which responses were blocked in a testosterone-treated fish was delayed and elongated (Figure 4B, right).

From the evoked potential traces, we calculated the normalized amplitude across stimulus delays and generated an inhibition curve (Figure 4C). We then divided the curve into onset and offset curves based on the point of minimum amplitude and fitted each curve to a sigmoid to determine two coefficients, slope, and inflection point (Figure 4D; see also STAR Methods). We found that the onset slope was flattened by testosterone (Figure 4E; $p = 0.0013$ for treatment, $p = 0.39$ for days after treatment, $p = 0.024$ for the interaction, linear model [LM]), while the

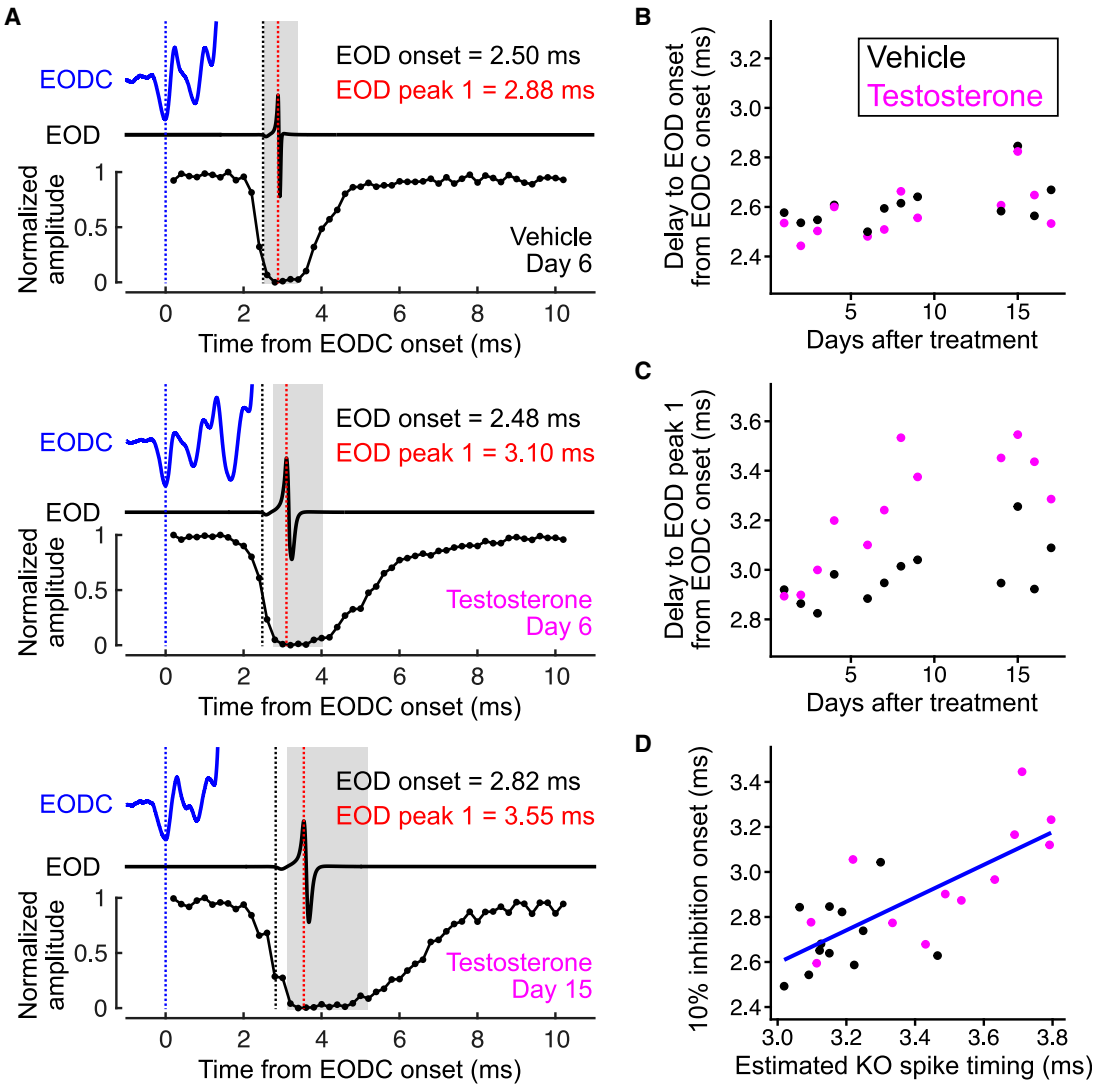

Figure 5. Shifted corollary discharge matches shifted reafferent spike timing

(A) Comparison of the time courses of the EOD command (EODC) (top blue traces), the EOD (middle trace), and corollary discharge inhibition. Vertical dotted lines indicate EODC onset (blue), EOD onset (black), and EOD peak 1 (red). Gray areas indicate 10% inhibition window calculated from the sigmoid curve fitting.

(B and C) Daily changes in EOD onset relative to EODC onset (B) and in EOD peak 1 relative to EODC onset (C). Each circle indicates individual fish (n = 12 for each treatment).

(D) Relationship between estimated KO spike timing and 10% inhibition onset. Regression line (blue) was determined using a linear model. The slope is 0.73 and the intercept is 0.41.

onset inflection point was not significantly affected (Figure 4F; $p = 0.15$ for treatment, $p = 0.15$ for days after treatment, $p = 0.89$ for the interaction, LM). By contrast, the offset slope was not significantly affected by testosterone (Figure 4G; $p = 0.25$ for treatment, $p = 0.40$ for days after treatment, $p = 0.35$ for the interaction, LM), but the offset inflection point was substantially delayed (Figure 4H; $p < 0.0001$ for treatment, $p = 0.0003$ for days after treatment, $p < 0.0001$ for the interaction, LM).

Shifted corollary discharge matches the shift in reafferent timing

We further examined whether the shifted corollary discharge was matched to the shifted reafferent input. Prior to evoked potential recording, we measured EOD timing relative to the EODC in unparalyzed fish to compare the time courses of corollary discharge and EOD production[32] (Figure 5A). We found no hormonally induced shift in EOD onset relative to the EODC (Figure 5B; $p = 0.36$ for treatment, $p = 0.0077$ for days after treatment, $p = 0.73$ for the interaction, LM). There was a slightly positive slope of onset versus day. The reason for this is unclear but may be due to the small amounts of ethanol used to dissolve the testosterone that were also provided to the vehicle treatment group. Importantly, the delay to EOD peak 1 from the EODC was shifted by testosterone (Figure 5C; $p < 0.0001$ for treatment, $p = 0.0001$ for days after treatment, $p = 0.046$ for the interaction, LM), demonstrating that EOD elongation indeed caused a shift in reafferent timing.

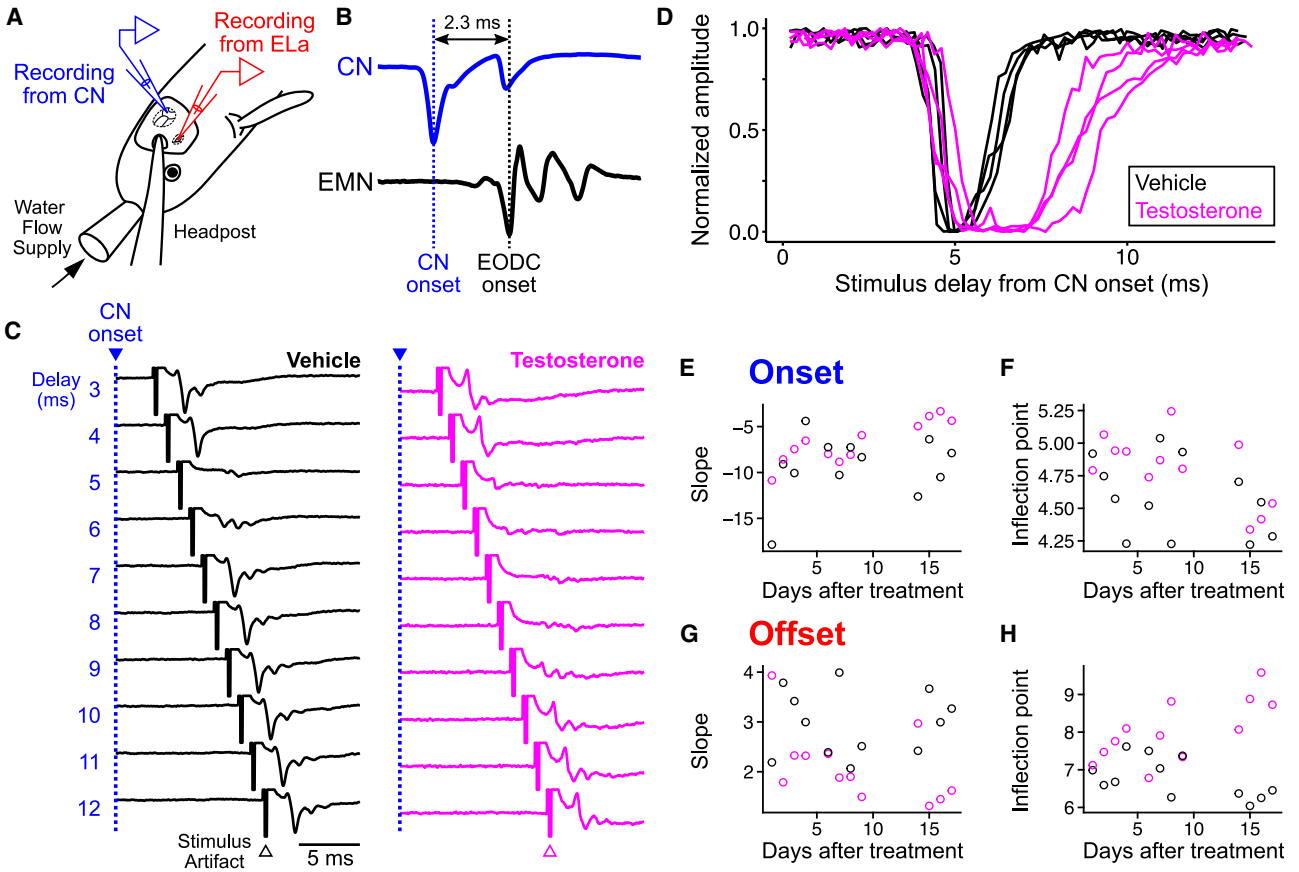

Figure 6. Testosterone alters corollary discharge without sensory feedback

(A) Measurement of corollary discharge timing from surgically silenced fish. Instead of EOD commands from EMNs, field potentials from the command nucleus (CN) in the hindbrain were used as a motor reference signal.

(B) Example traces of a CN potential and EOD command from an intact fish. The CN potential typically has a double negative peak and its onset was determined as the first negative peak. EOD command signals from the EMNs follow CN onset with a fixed delay in intact fish.

(C) Representative mean evoked potentials in response to stimuli at varying delays following the EOD command (3–12 ms) in vehicle- and testosterone-treated fish recorded 16 days after treatment.

(D) Corollary discharge inhibition curves in vehicle- and testosterone-treated, surgically silenced fish recorded 14–17 days after treatment.

(E–H) Changes in onset slope (E), inflection point of the onset (F), offset slope (G), and inflection point of the offset (H). Each circle indicates individual fish (n = 12 for each treatment).

See also Table S1.

Given the KO recording data, we estimated KO reafferent spike timing for these fish (Figure 3D; see also STAR Methods). We found that the timing of strong inhibition onset, or 10% inhibition onset, tightly correlated with the estimated KO reafferent spike timing (Figure 5D, $R = 0.75$, $p < 0.0001$). The slope and intercept of the regression line were 0.73 and 0.41, respectively.

Sensory feedback is not necessary for corollary discharge shift

How is the match between EOD elongation and corollary discharge shift achieved? One possibility is that the altered sensory feedback tunes corollary discharge timing through plasticity or learning. To test this, we made fish electrically silent by spinal cord transection and measured corollary discharge timing by recording evoked potentials.

Because the transection also eliminated EODCs from spinal EMNs, we recorded fictive EODs as field potentials from the CN in the hindbrain (Figure 6A), which fires one-to-one with EOD output in intact fish[34,35] (Figure 6B). CN activity was intact in all fish tested. Because CN potentials precede EODCs from the EMN in intact fish, the apparent inhibition window by corollary discharge was delayed, but the differences between vehicle and testosterone fish were similar to those of intact fish (Figures 6C and 6D).

As in intact fish, we found that testosterone flattened the onset slope (Figure 6E; $p = 0.025$ for treatment, $p = 0.024$ for days after treatment, $p = 0.253$ for the interaction, LM) and substantially delayed the offset inflection point (Figure 6H; $p < 0.0001$ for treatment, $p = 0.21$ for days after treatment, $p = 0.0008$ for the interaction, LM). However, unlike intact fish, the interaction effect on the onset slope was not significant. In addition, we found significant effects of testosterone on the onset inflection point (Figure 6F; $p = 0.043$ for treatment, $p = 0.023$ for days after treatment, $p = 0.60$ for the interaction,

LM) and on the offset slope (Figure 6G; p = 0.0057 for treatment, p = 0.25 for days after treatment, p = 0.17 for the interaction, LM), which were also different from the results in intact fish.

To statistically test whether the effects of testosterone were influenced by sensory feedback, we made additional models that included both intact and silent fish and added an additional independent variable, "silencing" (see also Table S1). We found no significant interaction effects between treatment and silencing nor between treatment, silencing, and days (Table S1), suggesting that absence of sensory feedback had little effect on the hormonal modulations. This indicates that altered sensory feedback is not necessary for driving this hormonally induced shift in corollary discharge timing. In these models, we found significant hormonal modulations, including gradual changes in onset slope (p = 0.0001 for treatment, p = 0.017 for the interaction between treatment and days) and offset inflection point (p < 0.0001 for treatment, p < 0.0001 for the interaction), and relatively rapid changes in onset inflection point (p = 0.012 for treatment, p = 0.61 for the interaction) and offset slope (p = 0.0054 for treatment, p = 0.10 for the interaction). We also found a significant interaction effect between surgery and days on onset inflection point (p = 0.007), suggesting that surgical silencing or an absence of sensory feedback might have slightly reduced the corollary discharge delay.

DISCUSSION

We found that testosterone modulates the timing of corollary discharge in a mormyrid fish (Figure 4). This modulation corresponds to the hormonally induced change in EOD duration that shifts the reafferent spike timing of electroreceptors (Figures 2, 3, and 5). Recordings from surgically silenced fish showed that exposure to sensory feedback is not necessary to drive this hormonal modulation of corollary discharge (Figure 6). These results suggest that testosterone directly and independently adjusts the internal signal that predicts the sensory consequences of peripheral motor output.

Changes in circulating steroid hormone levels can modulate motor systems,[2–6,36] sensory systems,[8–10] or both,[37,38] which is particularly evident in communication systems. These changes should alter the encoding of reafferent inputs, while the nervous system still faces the challenge of distinguishing between self and other. Corollary discharges from motor centers serve as predictive signals of the timing of motor output and mediate this discrimination in sensory processing across modalities and species.[24,39–41] Mismatch between sensory prediction and actual sensory feedback is associated with hallucinations in patients with schizophrenia.[42] Our results show that testosterone-treated mormyrid fish have modified a filter in their corollary discharge to match altered reafferent input (Figure 5). The onset of this filter occurs just prior to the peak timing of the reafferent spikes, and its longer duration can cover more variable spike timings, which were more often observed in testosterone-treated KOs (Figures 3, 4, and S1). As the task of self-other discrimination is ubiquitous across species and sensory modalities, we expect that hormonal shifts in corollary discharge will be found in a wider range of systems.[24,41]

To minimize mismatch throughout sensorimotor circuits, coordination of hormonal effects on different circuit components is essential. For example, in a gymnotiform electric fish that emits highly regular EODs, androgen treatment increases EOD duration while simultaneously decreasing EOD frequency in a coordinated manner.[36] Interestingly, localized androgen treatment of the electric organ increases EOD duration without affecting EOD frequency, suggesting independent regulation of EOD duration and frequency by androgens acting in the peripheral and central nervous systems, respectively, similar to our findings.[43] In addition, androgens directly lower the frequency tuning of electroreceptors in gymnotiforms,[37,44] in contrast to the indirect hormonal effect on KO receptors in mormyrid fish.[31]

We found that corollary discharge timing is regulated by circulating testosterone levels to achieve coordination of the electrocommunication circuit. Thus, one or more sites in the corollary discharge pathway may express androgen receptors. The corollary discharge originates in the CN and reaches the nELL via three additional nuclei, the bulbar command-associated nucleus (BCA), the mesencephalic command-associated nucleus (MCA), and the sublemniscal nucleus (slem)[21,23–25] (Figure 1B). A previous study examined androgen binding sites in the mormyrid brain but did not find binding sites in the corollary discharge pathway.[45] However, the examined area was limited to the relatively ventral side and likely missed parts of this corollary discharge pathway.[45] In addition, androgen binding sites may only become visible after testosterone treatment: a previous study using a gymnotiform fish showed that the expression of androgen receptors was upregulated following 15 days of hormone treatment.[46] Moreover, the actions of testosterone may be mediated by aromatase, which converts testosterone into estrogen.[47] Future studies should examine the distribution of both androgen and estrogen receptors throughout the corollary discharge pathway using testosterone-treated fish to identify where in the pathway they may be responsible for shifting corollary discharge timing.

The cellular mechanisms by which testosterone shifts corollary discharge timing remain to be determined. There are many possibilities. For example, testosterone, or estrogen produced by aromatase, may regulate γ-aminobutyric acid (GABA) transmission. In the first sensory center (nELL), primary KO afferents form excitatory, mixed chemical-electrical synapses onto the soma of adendritic nELL neurons, which in turn project to the midbrain (ELa).[26] The nELL neurons also receive inhibitory inputs from the slem neurons in the form of GABAergic boutons.[26] This inhibition functions to timeously block sensory responses to self-generated EODs, allowing the downstream pathway to selectively process EODs emitted by other fish.[23] Several studies have shown that testosterone or estrogen treatment can alter GABA receptor expression.[48,49] Thus, it is possible that testosterone directly affects GABA receptor expression in nELL neurons to change the kinetics of inhibitory synaptic currents, thus altering the time course of inhibition, resulting in a slower onset slope and delayed offset (Figures 4E and 4H; Table S1). However, we cannot exclude the possibility that testosterone acts on upstream nuclei in the corollary discharge pathway (BCA, MCA, and slem). Testosterone may change axonal morphology or myelination of neurons in these nuclei to delay action potential propagation and the timing of inhibition.[22,50–52] Testosterone

could also alter the passive or active electrical properties of neurons in this pathway to alter their excitability.[7,53,54] To determine which nucleus (or nuclei) contributes to the shift in corollary discharge timing, future studies can record command-related neural activities from these nuclei and compare their timing between testosterone- and vehicle-treated fish. Furthermore, a recent study documented changes in gene expression induced by testosterone in the electric organ of the same species of mormyrid we studied, many of which are likely associated with EOD elongation.[55] It will be interesting to determine whether similar molecular cascades underlie shifts in corollary discharge timing.

Altered sensory feedback itself could provide a basis for adjusting corollary discharge through plasticity. Such plasticity has been found in several systems, including passive and active electrolocation systems in mormyrid fish.[56–59] In these electrolocation systems, corollary discharge functions to subtract predictable sensory feedback from reafferent input by a modifiable efference copy, forming a "negative image" through cerebellum-like circuitry in the electrosensory lateral line lobe.[24,56,57] This negative image is formed at synapses between parallel fibers that carry corollary discharge inputs from the CN and medial ganglion cells that receive sensory inputs through spike-timing-dependent plasticity.[60–63] By contrast, in the communication pathway, we found that removal of sensory feedback had no effect on hormonal modulations of corollary discharge (Figures 4 and 6). However, we cannot conclude that sensory feedback has no effect on corollary discharge inhibition because we did not test whether altered sensory feedback is sufficient to modify corollary discharge inhibition. We observed very similar inhibition curves in intact and silent fish (Figures 4 and 6), but it is also possible that altered sensory feedback plays a key role in fine-tuning the onset of inhibition, which was fixed to KO spike timing in response to simulated reafferent input in intact fish (Figure 5). More localized treatment of testosterone in the electric organ, or other manipulations that alter sensory feedback over long periods of time without increasing systemic levels of testosterone, may allow us to test the effects of altered sensory feedback.

Coordinated changes in corollary discharge are essential for adaptive behavioral change, not only through hormonal plasticity but also through development or evolution, because all animals are constantly faced with the task of discriminating between self and others.[24,39–41] Coordination of behavioral change and a corollary discharge shift is also found in the diversification of communication signals among mormyrid species and in developmental changes in these signals within species.[32,64] A previous comparative study showed a correlation between EOD duration and the timing of corollary discharge inhibition onset, while the duration of corollary discharge inhibition was similar between and within species.[32] This evolutionary shift in corollary discharge inhibition contrasts with testosterone-treated fish having a significant elongation of the duration of corollary discharge inhibition. However, because the longer inhibition window could cancel the multiple spikes from KOs observed in testosterone-treated fish (Figure S1), both types of corollary discharge shifts appear to maintain a match between reafferent input timing and corollary discharge inhibition. It will be very interesting to test whether these evolutionary and developmental shifts share the same substrates or mechanisms responsible for the precise matching of corollary discharge and reafferent timing. Mormyrids are an excellent system to study sensorimotor coordination underlying plastic behavior and its relationship to evolutionary change.

STAR★METHODS

Detailed methods are provided in the online version of this paper and include the following:

- KEY RESOURCES TABLE
- RESOURCE AVAILABILITY
  - Lead contact
  - Materials availability
  - Data and code availability
- EXPERIMENTAL MODEL AND SUBJECT DETAILS
- METHOD DETAILS
  - Surgery for silencing the EOD
  - Hormone treatment
  - EOD recording
  - KO recording
  - EOD and EOD command recording
  - Evoked potential recording from intact fish
  - Evoked potential recording from silent fish
- QUANTIFICATION, STATISTICAL ANALYSIS AND DATA PRESENTATION

SUPPLEMENTAL INFORMATION

Supplemental information can be found online at https://doi.org/10.1016/j.cub.2023.06.069.

ACKNOWLEDGMENTS

This work was supported by the National Science Foundation (IOS-1755071 and IOS-2203122 to B.A.C.) and a Japan Society for the Promotion of Science Overseas Research Fellowship (202060318 to M.F.). We thank Martin W. Jarzyna for providing feedback on earlier versions of the manuscript and collecting data for Figure 6B and Mauricio Losilla for sharing the hormone treatment protocol.

AUTHOR CONTRIBUTIONS

Conceptualization, M.F. and B.A.C.; methodology, M.F. and B.A.C.; investigation, M.F.; formal analysis, M.F.; writing – original draft, M.F.; writing – review & editing, M.F. and B.A.C.; funding acquisition, M.F. and B.A.C.; supervision, B.A.C.

DECLARATION OF INTERESTS

The authors declare no competing interests.

Received: May 11, 2023
Revised: June 22, 2023
Accepted: June 28, 2023
Published: July 24, 2023

REFERENCES

1. Bass, A.H., and Hopkins, C.D. (1983). Hormonal control of sexual differentiation: changes in electric organ discharge waveform. Science *220*, 971–974.

2. Bleisch, W., Luine, V.N., and Nottebohm, F. (1984). Modification of synapses in androgen-sensitive muscle. I. Hormonal regulation of acetylcholine receptor number in the songbird syrinx. J. Neurosci. *4*, 786–792.
3. Sassoon, D.A., Gray, G.E., and Kelley, D.B. (1987). Androgen regulation of muscle fiber type in the sexually dimorphic larynx of Xenopus laevis. J. Neurosci. *7*, 3198–3206.
4. Modesto, T., and Canário, A.V.M. (2003). Hormonal control of swimbladder sonic muscle dimorphism in the Lusitanian toadfish Halobatrachus didactylus. J. Exp. Biol. *206*, 3467–3477.
5. Rhodes, H.J., Yu, H.J., and Yamaguchi, A. (2007). Xenopus vocalizations are controlled by a sexually differentiated hindbrain central pattern generator. J. Neurosci. *27*, 1485–1497.
6. Bass, A.H., and Remage-Healey, L. (2008). Central pattern generators for social vocalization: Androgen-dependent neurophysiological mechanisms. Horm. Behav. *53*, 659–672.
7. Meitzen, J., Weaver, A.L., Brenowitz, E.A., and Perkel, D.J. (2009). Plastic and stable electrophysiological properties of adult avian forebrain song-control neurons across changing breeding conditions. J. Neurosci. *29*, 6558–6567.
8. Caras, M.L. (2013). Estrogenic modulation of auditory processing: a vertebrate comparison. Front. Neuroendocrinol. *34*, 285–299.
9. Sisneros, J.A., Forlano, P.M., Deitcher, D.L., and Bass, A.H. (2004). Steroid-dependent auditory plasticity leads to adaptive coupling of sender and receiver. Science *305*, 404–407.
10. Yovanof, S., and Feng, A.S. (1983). Effects of estradiol on auditory evoked responses from the frog's auditory midbrain. Neurosci. Lett. *36*, 291–297.
11. Bennett, M.V.L. (1971). Electric organs. Fish Physiol. *5*, 347–491.
12. von der Emde, G. (1999). Active electrolocation of objects in weakly electric fish. J. Exp. Biol. *202*, 1205–1215.
13. Hopkins, C.D. (1999). Design features for electric communication. J. Exp. Biol. *202*, 1217–1228.
14. Hopkins, C.D. (1981). On the diversity of electric signals in a community of mormyrid electric fish in West Africa. Am. Zool. *21*, 211–222.
15. Carlson, B.A., Hopkins, C.D., and Thomas, P. (2000). Androgen correlates of socially induced changes in the electric organ discharge waveform of a mormyrid fish. Horm. Behav. *38*, 177–186.
16. Feulner, P.G.D., Plath, M., Engelmann, J., Kirschbaum, F., and Tiedemann, R. (2009). Electrifying love: electric fish use species-specific discharge for mate recognition. Biol. Lett. *5*, 225–228.
17. Moller, P. (1970). "Communication" in weakly electric fish, Gnathonemus niger (Mormyridae) I. Variation of electric organ discharge (EOD) frequency elicited by controlled electric stimuli. Anim. Behav. *18*, 768–786.
18. Bell, C.C., Myers, J.P., and Russell, C.J. (1974). Electric organ discharge patterns during dominance related behavioral displays in Gnathonemus petersii (Mormyridae). J. Comp. Physiol. *92*, 201–228.
19. Carlson, B.A. (2002). Electric signaling behavior and the mechanisms of electric organ discharge production in mormyrid fish. J. Physiol. Paris *96*, 405–419.
20. Carlson, B.A. (2009). Temporal-pattern recognition by single neurons in a sensory pathway devoted to social communication behavior. J. Neurosci. *29*, 9417–9428.
21. Baker, C.A., Kohashi, T., Lyons-Warren, A.M., Ma, X., and Carlson, B.A. (2013). Multiplexed temporal coding of electric communication signals in mormyrid fishes. J. Exp. Biol. *216*, 2365–2379.
22. Lyons-Warren, A.M., Kohashi, T., Mennerick, S., and Carlson, B.A. (2013). Detection of submillisecond spike timing differences based on delay-line anticoincidence detection. J. Neurophysiol. *110*, 2295–2311.
23. Bell, C.C., and Grant, K. (1989). Corollary discharge inhibition and preservation of temporal information in a sensory nucleus of mormyrid electric fish. J. Neurosci. *9*, 1029–1044.
24. Fukutomi, M., and Carlson, B.A. (2020). A history of corollary discharge: contributions of mormyrid weakly electric fish. Front. Integr. Neurosci. *14*, 42.
25. Bell, C.C., Libouban, S., and Szabo, T. (1983). Pathways of the electric organ discharge command and its corollary discharges in mormyrid fish. J. Comp. Neurol. *216*, 327–338.
26. Mugnaini, E., and Maler, L. (1987). Cytology and immunocytochemistry of the nucleus of the lateral line lobe in the electric fish Gnathonemus petersii (mormyridae): evidence suggesting that GABAergic synapses mediate an inhibitory corollary discharge. Synapse *1*, 32–56.
27. Bass, A.H. (1986). A hormone-sensitive communication system in an electric fish. J. Neurobiol. *17*, 131–155.
28. Bass, A.H., Denizot, J.P., and Marchaterre, M.A. (1986). Ultrastructural features and hormone-dependent sex differences of mormyrid electric organs. J. Comp. Neurol. *254*, 511–528.
29. Bass, A.H., and Volman, S.F. (1987). From behavior to membranes: testosterone-induced changes in action potential duration in electric organs. Proc. Natl. Acad. Sci. USA *84*, 9295–9298.
30. Freedman, E.G., Olyarchuk, J., Marchaterre, M.A., and Bass, A.H. (1989). A temporal analysis of testosterone-induced changes in electric organs and electric organ discharges of mormyrid fishes. J. Neurobiol. *20*, 619–634.
31. Bass, A.H., and Hopkins, C.D. (1984). Shifts in frequency tuning of electroreceptors in androgen-treated mormyrid fish. J. Comp. Physiol. *155*, 713–724.
32. Fukutomi, M., and Carlson, B.A. (2020). Signal diversification is associated with corollary discharge evolution in weakly electric fish. J. Neurosci. *40*, 6345–6356.
33. Bennett, M.V.L. (1971). Electroreception. Fish. Physiol. *5*, 493–574.
34. Grant, K., Bell, C.C., Clausse, S., and Ravaille, M. (1986). Morphology and physiology of the brainstem nuclei controlling the electric organ discharge in mormyrid fish. J. Comp. Neurol. *245*, 514–530.
35. Carlson, B.A. (2002). Neuroanatomy of the mormyrid electromotor control system. J. Comp. Neurol. *454*, 440–455.
36. Mills, A., and Zakon, H.H. (1987). Coordination of EOD frequency and pulse duration in a weakly electric wave fish: the influence of androgens. J. Comp. Physiol. *161*, 417–430.
37. Keller, C.H., Zakon, H.H., and Sanchez, D.Y. (1986). Evidence for a direct effect of androgens upon electroreceptor tuning. J. Comp. Physiol. A *158*, 301–310.
38. Zakon, H.H., Mills, A.C., and Ferrari, M.B. (1991). Androgen-dependent modulation of the electrosensory and electromotor systems of a weakly electric fish. Semin. Neurosci. *3*, 449–457.
39. von Holst, E., and Mittelstaedt, H. (1950). Das Reafferenzprinzip. Naturwissenschaften *37*, 464–476.
40. Sperry, R.W. (1950). Neural basis of the spontaneous optokinetic response produced by visual inversion. J. Comp. Physiol. Psychol. *43*, 482–489.
41. Crapse, T.B., and Sommer, M.A. (2008). Corollary discharge across the animal kingdom. Nat. Rev. Neurosci. *9*, 587–600.
42. Abram, S.V., Hua, J.P.Y., and Ford, J.M. (2022). Consider the pons: bridging the gap on sensory prediction abnormalities in schizophrenia. Trends Neurosci. *45*, 798–808.
43. Few, W.P., and Zakon, H.H. (2001). Androgens alter electric organ discharge pulse duration despite stability in electric organ discharge frequency. Horm. Behav. *40*, 434–442.
44. Ferrari, M.B., and Zakon, H.H. (1989). The medullary pacemaker nucleus is unnecessary for electroreceptor tuning plasticity in Sternopygus. J. Neurosci. *9*, 1354–1361.
45. Bass, A.H., Segil, N., and Kelley, D.B. (1986). Androgen binding in the brain and electric organ of a mormyrid fish. J. Comp. Physiol. A *159*, 535–544.
46. Pouso, P., Quintana, L., Bolatto, C., and Silva, A.C. (2010). Brain androgen receptor expression correlates with seasonal changes in the behavior of a weakly electric fish, Brachyhypopomus gauderio. Horm. Behav. *58*, 729–736.

47. Balthazart, J., and Ball, G.F. (1998). New insights into the regulation and function of brain estrogen synthase (aromatase). Trends Neurosci. *21*, 243–249.

48. Herbison, A.E. (1997). Estrogen regulation of GABA transmission in rat preoptic area. Brain Res. Bull. *44*, 321–326.

49. Zhang, L., Chang, Y.H., Feldman, A.N., Ma, W., Lahjouji, F., Barker, J.L., Hu, Q., Maric, D., Li, B.S., Li, W., et al. (1999). The expression of GABAA receptor $\alpha 2$ subunit is upregulated by testosterone in rat cerebral cortex. Neurosci. Lett. *265*, 25–28.

50. Carr, C.E., and Konishi, M. (1988). Axonal delay lines for time measurement in the owl's brainstem. Proc. Natl. Acad. Sci. USA *85*, 8311–8315.

51. Milner, T.A., and Loy, R. (1982). Hormonal regulation of axonal sprouting in the hippocampus. Brain Res. *243*, 180–185.

52. Bielecki, B., Mattern, C., Ghoumari, A.M., Javaid, S., Smietanka, K., Abi Ghanem, C.A., Mhaouty-Kodja, S., Ghandour, M.S., Baulieu, E.E., Franklin, R.J.M., et al. (2016). Unexpected central role of the androgen receptor in the spontaneous regeneration of myelin. Proc. Natl. Acad. Sci. USA *113*, 14829–14834.

53. Zakon, H.H. (1998). The effects of steroid hormones on electrical activity of excitable cells. Trends Neurosci. *21*, 202–207.

54. Kohashi, T., and Carlson, B.A. (2014). A fast BK-type KCa current acts as a postsynaptic modulator of temporal selectivity for communication signals. Front. Cell. Neurosci. *8*, 286.

55. Losilla-Lacayo, M. (2021). Genomic basis of eelectric signal variation in African weakly electric fish. PhD thesis (Michigan State University).

56. Sawtell, N.B., Williams, A., and Bell, C.C. (2005). From sparks to spikes: information processing in the electrosensory systems of fish. Curr. Opin. Neurobiol. *15*, 437–443.

57. Sawtell, N.B. (2017). Neural mechanisms for predicting the sensory consequences of behavior: insights from electrosensory systems. Annu. Rev. Physiol. *79*, 381–399.

58. Singla, S., Dempsey, C., Warren, R., Enikolopov, A.G., and Sawtell, N.B. (2017). A cerebellum-like circuit in the auditory system cancels responses to self-generated sounds. Nat. Neurosci. *20*, 943–950.

59. Perks, K.E., Krotinger, A., and Bodznick, D. (2020). A cerebellum-like circuit in the lateral line system of fish cancels mechanosensory input associated with its own movements. J. Exp. Biol. *223*, jeb204438.

60. Bell, C.C., Caputi, A., Grant, K., and Serrier, J. (1993). Storage of a sensory pattern by anti-Hebbian synaptic plasticity in an electric fish. Proc. Natl. Acad. Sci. USA *90*, 4650–4654.

61. Bell, C.C., Han, V.Z., Sugawara, Y., and Grant, K. (1997). Synaptic plasticity in a cerebellum-like structure depends on temporal order. Nature *387*, 278–281.

62. Kennedy, A., Wayne, G., Kaifosh, P., Alviña, K., Abbott, L.F., and Sawtell, N.B. (2014). A temporal basis for predicting the sensory consequences of motor commands in an electric fish. Nat. Neurosci. *17*, 416–422.

63. Muller, S.Z., Zadina, A.N., Abbott, L.F., and Sawtell, N.B. (2019). Continual learning in a multi-layer network of an electric fish. Cell *179*, 1382–1392.e10.

64. Paul, C., Mamonekene, V., Vater, M., Feulner, P.G.D., Engelmann, J., Tiedemann, R., and Kirschbaum, F. (2015). Comparative histology of the adult electric organ among four species of the genus Campylomormyrus (Teleostei: Mormyridae). J. Comp. Physiol. A Neuroethol. Sens. Neural Behav. Physiol. *201*, 357–374.

65. Moller, P. (1976). Electric signals and schooling behavior in a weakly electric fish, Marcusenius cyprinoides L. (Mormyriformes). Science *193*, 697–699.

66. Lyons-Warren, A.M., Hollmann, M., and Carlson, B.A. (2012). Sensory receptor diversity establishes a peripheral population code for stimulus duration at low intensities. J. Exp. Biol. *215*, 2586–2600.

67. Baker, C.A., Huck, K.R., and Carlson, B.A. (2015). Peripheral sensory coding through oscillatory synchrony in weakly electric fish. eLife *4*, e08163.

STAR★METHODS

KEY RESOURCES TABLE

REAGENT or RESOURCE	SOURCE	IDENTIFIER
Chemicals, peptides, and recombinant proteins		
Tricaine methanesulfonate (MS-222)	Western Chemical Inc	NC0242409; CAS: 886-86-2
Lidocaine	Sigma-Aldrich	L7757; CAS: 137-58-6
17α-methyltestosterone	Sigma-Aldrich	M7252; CAS: 58-18-4
Gallamine triethiodide (Flaxedil)	Sigma-Aldrich	G8134; CAS: 65-29-2
Experimental models: organisms/strains		
Brienomyrus brachyistius	Bailey's Tropical Fish, AliKhan Tropical Fish	N/A
Software and algorithms		
MATLAB 2012a	The Mathworks	https://www.mathworks.com/product/matlab.html
R version 4.0.3	R Core Team	https://www.r-project.org/

RESOURCE AVAILABILITY

Lead contact

Further information and requests for resources and reagents should be directed to and will be fulfilled by the Lead Contact, Bruce A. Carlson (carlson.bruce@wustl.edu).

Materials availability

This study did not generate new unique reagents, strains, or lines.

Data and code availability

- The datasets supporting the current study are available from the lead contact upon request.
- The original codes are available from the lead contact upon request.
- Any additional information required to reanalyze the data reported in this paper is available from the lead contact upon request.
- The datasets supporting the current study have not been deposited in a public repository but are available from the corresponding author on request.

EXPERIMENTAL MODEL AND SUBJECT DETAILS

We used a total of 54 *Brienomyrus brachyistius* of both sexes in non-reproductive state (5.4–10.9 cm in standard length). All fish were purchased from Bailey Wholesale Tropical Fish or Alikhan Tropical Fish. The fish were housed in groups with a 12 h: 12 h light/dark cycle, temperature of 25–29°C, pH of 6–7, and water conductivity of 200–400 μS/cm. Fish were fed live black worms or frozen blood worms four times per week. All procedures were in accordance with guidelines established by the National Institutes of Health and were approved by the Animal Care and Use Committee at Washington University in St. Louis.

Half of the fish were testosterone treated and the other half were vehicle treated. All experiments below used the same number of fish for each treatment. Six fish were used for KO recording. Another twenty-four fish were used for simultaneous recording of EOD and EODC and evoked potential recording from ELa. For 8 of these fish, the change in EOD was followed up to 13 days after the start of treatment. The remaining 24 fish were surgically silenced to eliminate EOD production by spinal cord transection before treatment, and then used for evoked potential recording.

METHOD DETAILS

Surgery for silencing the EOD

Fish were anesthetized in a solution of 300 mg/L MS-222 (Western Chemical Inc.). When movement ceased, the fish were removed from the solution and 70% ethanol was applied around the incision site, just anterior to the electric organ. A 26-gauge needle was

then inserted through the skin to transect the spinal cord. After transection, lidocaine (0.2% solution; Sigma-Aldrich) was applied around the incision site, but not directly at the incision site, for local anesthesia. Finally, the incision was closed with a small amount of superglue and the fish was returned to its home tank. This operation did not affect motility, as the spinal motorneurons controlling movement are all located anterior to the incision site.[31,65] Prior to treatment, surgically silenced fish were allowed to recover in isolation for at least 6 days.

Hormone treatment

A treatment tank (25.4 * 30.5 * 50.8 cm) was prepared for each treatment group, divided into four compartments with mesh panels, and filled with 30 L of treated aquarium water. For testosterone fish, 60 mg of solid 17α-methyltestosterone (Sigma-Aldrich) dissolved in 0.4 mL 95% ethanol was added to the testosterone tank on the start day and the next day, and then every two days thereafter. For vehicle fish, only 0.4 mL 95% ethanol was added to the vehicle tank on the same schedule as the testosterone treatment. Except for the treatment and separation with mesh panels, tank conditions were identical to our normal fish housing.

EOD recording

EOD recordings were made from freely swimming fish prior to EOD and EODC recording or KO recording in intact fish. EODs were amplified 10 times, bandpass filtered (1 Hz–50 kHz) (BMA-200, CWE), digitized at a rate of 195 kHz (RP2.1, Tucker-Davis Technologies), and stored using custom software in MATLAB (The MathWorks). From the recorded EOD waveform, we determined EOD onset as the point crossing 20% of peak 0 amplitude and EOD offset as the point crossing zero after peak 2. EOD duration was determined as the period between EOD onset and offset. Delay to peak 1 was determined as the period between EOD onset and timing of peak 1. Peak power frequency was calculated by fast Fourier transformation. Each value was calculated from 10 EODs obtained from each fish, and the average was used for analysis.

KO recording

The recording method was similar to previous studies.[66,67] Recordings were performed on 1, 2, 4, 6, 7, 9, 14, 15, and 17 days after starting treatment. Fish were anesthetized with a solution of 300 mg/L MS-222, and then paralyzed and electrically silenced with 50–60 μL of 0.05 mg/mL gallamine triethiodide (Flaxedil, Sigma-Aldrich). The fish were then placed on a plastic platform with lateral supports in a recording chamber (20 * 12.5 * 45 cm) filled with freshwater covering the entire body of the fish and were respirated with aerated freshwater through a pipette tip placed in the fish's mouth. To verify that the fish had recovered from anesthesia, field potentials were recorded from EMNs using a pair of electrodes placed next to the fish's tail. After recovery, indicated by EOD commands from the EMNs, the recording session was started. After recording, the fish were allowed to fully recover from paralysis before being returned to their home tank.

We made recording electrodes from borosilicate capillary glass (o.d. = 1 mm, i.d. = 0.5 mm; Model 626000, A-M Systems). Using a Bunsen burner, we bent the last ∼1–2 cm to a ∼10–30-degree angle and polished the tip. The electrode was filled with tank water, placed in an electrode holder with a Ag-AgCl wire connected to the headstage of an amplifier (Neuroprove Model 1600, A-M Systems) and positioned over individual KOs without touching them. The extracellular activity was referenced to ground, amplified 10 times and low-pass filtered (cut-off frequency = 10 kHz) with the amplifier, and digitized at a sampling rate of 97.7 kHz (RP2.1, Tucker-Davis Technologies). Electrosensory stimuli were generated at a sampling rate of 195.31 kHz (RP2.1, Tucker-Davis Technologies), attenuated (PA5, Tucker-Davis Technologies), and delivered through the recording electrode as constant-current stimuli. We used a bridge balance to minimize stimulus artifact. Recording traces were stored using custom MATLAB (The MathWorks) software from 20 ms before stimulation to 20 ms after stimulation.

We used an inverted (or head-negative) EOD waveform for stimulation, which was recorded from the same individual just prior to recording. When a fish generates an EOD, all the KOs on its skin receive the same-direction currents consisting of a large outward current followed by a large inward current. This waveform is opposite to the waveform obtained when a recording electrode is placed at the head and a reference electrode is placed at the tail. We tested each KO with at least two different stimulus intensities, with a 5 dB attenuation interval, including one intensity where KO spike amplitude exceeded the stimulus artifact and one where it did not. We presented 50 repetitions for each stimulus intensity.

For each recording, we selected the maximum stimulus intensity at which spikes could be reliably distinguished from artifact for further analysis. Spikes were detected by finding the peak voltage that crossed a manually set threshold specific to each KO. For some KOs, a stimulus artifact template was created by taking the median trace of non-responsive traces to weaker stimuli and scaling it. The template trace was subtracted from the recording traces to stronger stimuli and spikes were detected by the threshold crossing method.

We computed the spike density function (SDF) by convolving each KO spike time with a Gaussian of 0.1 ms width and then averaging over stimulus repetitions. We first determined the timing of the largest peak for each KO SDF trace as the first peak. KO peak latency was calculated as the interval between EOD stimulus onset and the time of the first peak. KO peak latency to EOD peak 1 was calculated as the interval between the time of EOD peak 1 and the time of the first peak.

When looking at the distribution of KO peak latency to EOD peak 1, two obvious outliers were found. These KO recordings showed weak responses to the stimuli and were excluded. As a result, a total of 72 recordings from 32 different KOs were used for the subsequent statistical analyses. Note that the 23 out of 32 KOs could be recorded on multiple days.

We also determined the timing of the second largest peak for each SDF trace as the second peak. The z-score of the second peak was calculated using the z-score over each SDF.

EOD and EOD command recording

Recording and analysis methods were similar to a previous study.[32] Recordings were performed before evoked potential recording on 1, 2, 3, 4, 6, 7, 8, 9, 14, 15, 16, and 17 days after starting treatment. Fish were anesthetized in a solution of 300 mg/L MS-222 (Sigma Millipore) and placed on a plastic platform with lateral supports in the recording chamber filled with freshwater covering the entire body of the fish. Fish were restrained by lateral plastic pins, a plastic tube on the tail, and two or three folded paper towels on the dorsal skin surface. EOD commands from spinal EMNs were recorded with a pair of electrodes located within the plastic tube and oriented parallel to the fish's electric organ, amplified 1000×, and bandpass filtered (10 Hz to 5 kHz) (Model 1700, A-M Systems). While EOD commands from EMNs were recorded, the EODs were recorded by separate electrodes, amplified 10 times, and bandpass filtered (1 Hz to 50 kHz) (BMA-200, CWE). These recordings were digitized at a rate of 1 MHz and saved (TDS 3014C, Tektronix).

EOD command traces from EMNs were averaged across trials, and EOD traces were filtered by a 21st-order median filter whose time window was 0.02 ms and averaged across trials. EOD onset was determined in the same way we determined EOD onset in freely swimming EOD recordings. EOD command onset was determined as the first negative peak in the averaged EMN trace. Delay to EOD onset was calculated as the time between EOD command onset and EOD onset. Delay to EOD peak 1 from the EOD command was calculated as the sum of the delay to EOD onset and the delay between EOD onset and peak 1 recorded from freely swimming fish.

Evoked potential recording from intact fish

The recording and analysis methods were similar to a previous study.[20,22,32] Recordings were performed on 1, 2, 3, 4, 6, 7, 8, 9, 14, 15, 16, and 17 days after starting treatment. Fish were anesthetized with a solution of 300 mg/L MS-222, and then paralyzed with 0.05–0.1 mL of 3.0 mg/mL Flaxedil. The fish were then transferred to a recording chamber filled with water and positioned on a plastic platform, leaving a small region of the head above water level. During surgery, we maintained general anesthesia by respirating the fish with an aerated solution of 100 mg/ml MS-222 through a pipette tip placed in the mouth. For local anesthesia, we applied 0.2% lidocaine on the skin overlying the incision site, and then made an incision to uncover the skull overlying the ELa. Next, we glued a headpost to the skull before using a dental drill and forceps to remove a rectangular piece of skull covering the ELa. After exposing ELa, we placed a reference electrode on the nearby cerebellum. Following surgery, we switched respiration to fresh water and allowed the fish to recover from general anesthesia. EOD commands were also recorded from the EMNs and sent to a window discriminator for time stamping (SYS-121, World Precision Instruments). At the end of the recording session, the respiration of the fish was switched back to 100 mg/L MS-222 until no EOD commands could be recorded, and then the fish was euthanized by freezing.

Recording electrodes (Model 626000, A-M Systems) were pulled with a micropipette puller (Model P-97, Sutter Instrument), broken to a tip diameter of 10–20 μm, and filled with 3 M NaCl solution. Evoked field potentials were amplified 1000×, bandpass filtered (10 Hz–5 kHz) (Model 1700, A-M Systems), digitized at a rate of 97.7 kHz (RX8, Tucker-Davis Technologies), and stored using custom software in MATLAB (The MathWorks). We presented 0.2 ms bipolar square pulses at several delays following the EOD command onset, typically ∼0.2–10.2 ms with 0.2 ms intervals, in a randomized order. The stimulus intensity was fixed at 73.6 mV/cm. Each delay was repeated 10 times.

Technically, the window discriminator could not detect the minimum point of the first negative peak in the EOD command, but rather the point at which a manually selected threshold was crossed. Therefore, we also recorded the EOD command and the digital output of the window discriminator to measure the stimulus delay to EOD command onset. Using this, the corrected stimulus delay was used in the subsequent analyses.

To characterize corollary discharge inhibition, we first calculated the normalized amplitude by the following steps: (i) calculating the peak-to-peak (PP) amplitude 2–4 ms after stimulus onset for each stimulus delay, (ii) subtracting the minimum PP amplitude across all delays, and (iii) dividing by the difference between the maximum PP amplitude and the minimum PP amplitude. Sigmoid curve fitting was then applied to the normalized amplitude curve as follows: (i) determining the minimum point and dividing into onset and offset directions, (ii) selecting the points ranging from the minimum amplitude point to a point above 50% amplitude where the next point is lower than that point for the first time for each direction, and (iii) fitting the following expression:

$$Normalized\ amplitude = \frac{1}{1+e^{slope \times (inflection\ point - Stimulus\ delay)}}$$

where slope and inflection point are the coefficients of this curve. The coefficients of the onset curve were used to calculate 10% onset and offset.

Evoked potential recording from silent fish

Recordings were performed on 1, 2, 3, 4, 6, 7, 8, 9, 14, 15, 16, and 17 days after starting treatment. The procedure was almost the same as in intact fish, but EOD commands from the EMNs were silent because the spinal cord had been cut anterior to the electric organ. As an alternative motor reference signal, we recorded field potentials from the command nucleus (CN) in the hindbrain. Before exposing ELa, we made a second incision window in the skull on the dorsal surface above the CN. After recovery from anesthesia, we

searched for a CN potential using another electrode controlled by a motorized micromanipulator (MP-285, Sutter Instrument). CN typically exhibited a double negative potential, and the onset was determined as the first negative peak. Field potential signals from the CN were processed in the same way as EOD command recording from the EMNs to trigger electrosensory stimuli. Since the CN onset preceded the EMN onset, a wider range of stimulus delay to the command (~0.2–13.2 ms with 0.2 ms intervals) was used. The stimulus delay from the CN field potential was also measured and the corrected stimulus delay was used in the analyses.

Our recordings of command-related potentials from the hindbrain possibly include the medullary relay nucleus that is immediately dorsal to the CN. Technically, it was difficult to accurately distinguish between these nuclei without the EMN reference. Because these nuclei are electrically coupled and have a very small difference in peak timing relative to the EMN in intact fish,[34,35] we analyzed the recordings without distinguishing between them.

QUANTIFICATION, STATISTICAL ANALYSIS AND DATA PRESENTATION

We performed all statistical tests using R version 4.0.3. Additional details on sample sizes and statistical tests can be found in figure legends and the main text. We used the nlme package to make a model that accounts for random effects. To assess hormonal effects on EOD duration, peak power frequency and delay to EOD peak 1, we made linear mixed models in which the fixed effects were treatment (vehicle or testosterone), days after treatment, and the interaction, and the random effect was individual fish (Figures 2B–2D). To assess the hormonal effects on KO peak latency, we made a linear mixed model in which the fixed effects were treatment, days after treatment, and the interaction, and the random effect was individual KO (Figure 3C). To assess the hormonal effects on the corollary discharge inhibition curves (Figures 4 and 6) and EOD timing relative to the EOD command onset (Figures 5B and 5C), we made linear models with fixed effects of treatment, days after treatment, and the interaction. Additionally, we also made linear models with fixed effects of treatment, surgery, days after treatment, and the interactions (Table S1). To test for significant effects, we applied an analysis of variance to these models. To describe the relationship between delay to EOD peak 1 and KO peak latency (Figure 3D) or KO peak latency to EOD peak 1 (Figure 3E), we made a linear mixed model in which the fixed effect was delay to EOD peak 1 and the random effect was individual KO and determined the slope and intercept of the regression line. In this case, we tested whether a given parameter was significantly different from zero. Using the coefficients from Figure 3D, we estimated KO spike timing of fish (intact) that were used for evoked potential recording (Figure 5D). To determine the relationship between estimated KO spike timing, we calculated the Pearson's correlation coefficient.